ELSEVIER

Catalysis Today 62 (2000) 209–217

CATALYSIS TODAY

www.elsevier.com/locate/cattod

Catalytic combustion of methane on Pd–Cu/SiO_2 catalysts

P. Reyes [a,*], A. Figueroa [a], G. Pecchi [a], J.L.G. Fierro [b]

[a] *Facultad de Ciencias Químicas, Universidad de Concepción, Casilla 160-C, Concepción, Chile*
[b] *Instituto de Catálisis y Petroleoquímica, CSIC, Madrid, Spain*

Abstract

Different series of Pd/SiO_2, Pd–Cu/SiO_2 and Cu/SiO_2 catalysts prepared by the sol–gel method and by impregnation on a commercial silica were investigated. The solids were characterised by evaluating the surface area, porosity, metal dispersion and surface composition. The activity for the combustion of methane was measured under stoichiometric and oxidant conditions. In all the samples, the excess of oxygen shifts the conversion of methane towards lower temperatures. In the impregnated series, copper reduces the activity due to a copper–palladium interaction, which modifies the nature of the active site. In the sol–gel catalysts the main effect produced by the presence of copper is to modify the porosity of the solid, generating catalysts with high microporosity. The presence of micropores limits the access of the reactant to the active site, which makes catalyst activity lower. In addition, the sol–gel catalyst subjected to stringent reaction conditions exhibited an activity enhancement due to the development of some mesoporosity. On the contrary, a slight deactivation was observed in the impregnated Pd–Cu catalysts as a consequence of metal sinterisation.

Keywords: Palladium; Copper; Methane; Combustion

1. Introduction

The catalytic combustion is one of the several industrial processes for pollution abatement. Catalysts able to perform combustion are divided into two groups: noble metals for which reactions may start at temperatures as low as room temperature and transition metal oxides which are less efficient, but usually also more resistant towards high temperatures. Regarding the noble metal supported catalysts, most of the studies have been focused on platinum and palladium [1,2]. The superior performance of palladium as a catalyst for the complete oxidation to carbon dioxide and water has been well known for years [3,4]. The nature of the active sites at temperatures below 500°C where catalytic oxidation is initiated, has also been the subject of numerous studies [5,6]. The nature of the support has also been investigated, being Al_2O_3, SiO_2–Al_2O_3, SiO_2, ThO_2, ZrO_2, SnO_2 and TiO_2, among others extensively studied [7–9]. The sinterisation of the metal component is an important problem in treatments of industrial emissions. This is caused not only by the presence of steam in the reaction stream but also by exposing the catalysts to high temperatures. In certain combustion processes the catalyst still works after being subjected to temperatures as high as 1000°C. Migration of the metal crystallites in the presence of steam may be minimised by using catalysts prepared by the sol–gel method. In fact, one of the advantages reported for the sol–gel method in the preparation of metallic catalysts is that the sintering is highly restricted because the metal component is strongly interacting with the support and, in some cases, remains buried into the support [10,11]. In the last 20 years bimetallic catalysts have received the attention

* Corresponding author. Fax: +56-41-245974.
E-mail address: preyes@udec.cl (P. Reyes).

0920-5861/00/$ – see front matter
PII: S0920-5861(00)00422-3

of number of investigations. The addition of a second metal to a noble metal supported catalyst has allowed to improve the activity, selectivity and stability of different catalyst. In some studies the aim of the presence of the second metal is to minimise the poisoning of the active metal. This is especially interesting if the feed contains certain amounts of substances able to poison the active phase. Therefore, the second metal having a strong interaction with the poison molecule should de chosen. Thus in the presence of sulphur molecules, the addition of Cu to Pd or Pt catalysts minimise the deactivation of the solids during methane combustion [12].

In the present work two different series of Pd/SiO_2 and $Pd–Cu/SiO_2$ catalysts containing 0.5 wt.% Pd and different Cu loading (from 0.3 to 1.2 wt.%) were prepared. One of the series was prepared by the sol–gel method using tetraethoxysilane, $Pd(acac)_2$ and $Cu(NO_3)_2$ as precursors of SiO_2, Pd and Cu, respectively. According to previous studies, a pH of gelation of 5, using acetic acid as hydrolysis agent, was chosen [13]. The other series was prepared by impregnation or co-impregnation of the same precursors on a commercial silica. The catalysts were characterised by nitrogen adsorption at 77 K, H_2-chemisorption measurements at 343 K, TEM studies for particle size evaluation, and XPS analysis to determine the surface composition and the chemical state of the metal components. The combustion of methane with a stoichiometric and an excess of oxygen was investigated.

2. Experimental

2.1. Catalysts preparation

Two different series of Pd/SiO_2, $Pd–Cu/SiO_2$ and Cu/SiO_2 catalysts, containing 0.5 wt.% Pd and variable amounts of Cu ranging from 0.3 to 1.2 wt.%, were prepared. One series was prepared by impregnation of a commercial SiO_2 (BASF D11-11, $S_{BET} = 154\,m^2\,g^{-1}$) with an aqueous solution of copper nitrate at 308 K. The dried impregnate was then calcined in air at 673 K for 4 h. For the binary catalysts, the Cu/SiO_2 samples were subsequently impregnated with a toluene solution of $Pd(acac)_2$ at 308 K. The other series was prepared using the sol–gel method. Basically, the silica precursor, tetraethylorthosilicate (TEOS), was gelated in the presence of ethanol, water, $Pd(acac)_2$ and/or copper nitrate at 353 K at pH of 5. The pH was adjusted using CH_3COOH. The gel so obtained was then dried at 343 K overnight and finally calcined in air at 673 K for 4 h. The reduction was carried out in situ for 1 h at 773 K.

2.2. Characterisation

Specific area and porosity were obtained from nitrogen adsorption at 77 K in a Micromeritics Model Gemini 2370. Hydrogen chemisorption measurements at 343 K were carried out in a greaseless volumetric system to evaluate the hydrogen uptake and H/Pd ratio. Before the chemisorption experiment, the samples were reduced in situ at 773 K for 2 h and then outgassed for 4 h at the same temperature. TEM was used for the observation of the supported palladium particles. These experiments were performed in a JEOL Model JEM-1200 EX II instrument. The samples were prepared by the extractive replica procedure. TPR experiments were carried out in a TPR/TPD 2900 Micromeritics system provided with a thermal-conductivity detector. The reducing gas was a mixture of 5% H_2/Ar ($40\,cm^3\,min^{-1}$) and a heating rate of $10\,K\,min^{-1}$. XP spectra were recorded using an Escalab 200R spectrometer provided with a hemispherical analyser working in a constant pass energy mode and Mg Kα X-ray radiation ($h\nu = 1253.6$ eV), operated at 10 mA and 12 kV. The surface Pd/Cu and Cu/Si ratios were estimated from the integrated intensities of Pd $3d_{5/2}$, Si 2p and Cu $2p_{3/2}$ peaks, after background subtraction, and corrected by the atomic sensitivity factors [14]. The Si 2p line at 103.4 eV was taken as an internal standard for binding energy (BE) measurements. Palladium and copper peaks were decomposed into several components assuming that the peaks had Gaussian–Lorentzian shapes.

2.3. Catalytic measurements

The catalytic activity in the combustion of methane was evaluated in a conventional flow reactor at atmospheric pressure. In each experiment 200 mg of catalysts were used. The calcined samples were reduced in situ in flowing H_2 ($50\,cm^3\,g^{-1}$) up to 773 K for 1 h. Then the samples were cooled down to 473 K and the reducing gas was switched to He as the

carrier. After 30 min of stabilisation at this temperature, the carrier gas was switched to the reactant gaseous CH_4:O_2:He = 1:2:97 (molar) mixture and the cycle of combustion was performed. To evaluate the catalytic behaviour of each series, the reaction was studied under stoichiometric and oxidant conditions. In the studied oxidant conditions the composition of the reactant mixture CH_4:O_2:He = 1:4:95 was used. The activity was measured at different temperatures from 473 up to the temperature required for a total conversion. A heating rate of 1 K min^{-1} was used in all the experiments. The effluents of the reactor were analysed by an on-line gas chromatograph. A single column containing molecular sieve (5A) was used and the chromatographic separation was carried out isothermally at 333 K with helium as carrier gas. In some experiments a Quadruple Mass Spectrometer Hiden HPT 20 was used to detect small traces of products.

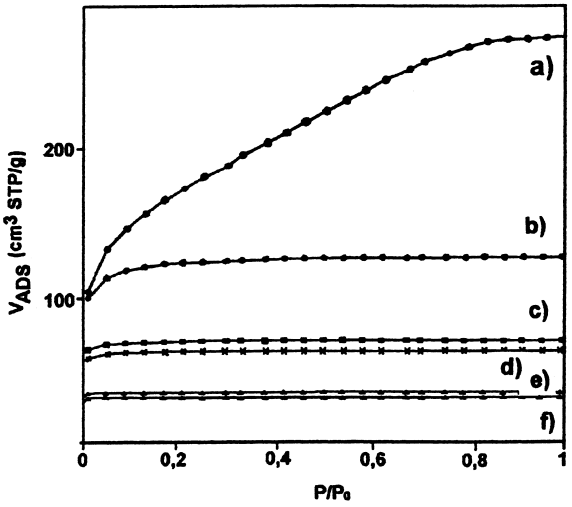

Fig. 1. Nitrogen adsorption isotherms at 77 K for the sol–gel Pd–Cu/SiO_2 catalysts. (a) 0.5Pd/SiO_2; (b) 0.5Pd–0.3Cu/SiO_2; (c) 0.5Pd–0.4Cu/SiO_2; (d) 0.5Pd–0.6Cu/SiO_2; (e) 0.5Pd–1.2Cu/SiO_2; (f) 1.0Cu/SiO_2.

3. Results and discussion

The shape of nitrogen adsorption isotherms at 77 K was quite different in the two catalyst series. The series prepared by impregnation of the metal precursor on commercial silica showed isotherms belonging to a type IV of the BDDT classification, with almost no change in the extent of adsorption with the metal loading. In fact, the specific area obtained for the catalysts prepared by impregnation was similar to that of the support (154 m^2 g^{-1}). On the other hand, in the catalysts prepared by the sol–gel procedure, in which the co-gelation of silica and metal precursors is carried out, the shape of the adsorption isotherms is mainly type I, indicative of microporous solids. This fact may be explained considering that the gelation in the presence of copper nitrate precursor, which is dissociated in solution, can be strongly adsorbed on nucleophiles such as $\equiv$Si–O^- during the condensation process [15]. Hence, the ionic interaction between the metal precursor ion and the nucleophilic, present during the gelation reaction, may lead to a highly branched polymeric product, responsible of the micropore structure. The only exception in this series is the Pd/SiO_2 catalysts in which a significant proportion of both micro and mesopores are present. This behaviour is explained taking into account that, during the gelation of this solid, a non-ionic metal precursor was used ($Pd(acac)_2$). Fig. 1 displays the nitrogen adsorption isotherms for the sol–gel catalysts, and Table 1 summarises specific area, pore volume, percent of micropore volume, and average pore diameter for all the studied catalysts.

TPR experiments were run in the temperature range from 195 to 775 K, and the profiles of the calcined samples are displayed in Fig. 2A and B. In all cases, a single peak centred around 293 K, which may be attributed to the reduction of PdO, is observed. As this reduction occurs at temperatures close to room temperature, it appears that palladium is well dispersed. In addition, a negative peak around 350 K, associated to the decomposition of a bulk palladium hydride, is also observed. This also may be assigned as desorption of H_2 molecules adsorbed on the surface of Pd [16,17]. With regard to the reduction of copper oxide species, Robertson et al. [18] have reported that the reduction of Cu/SiO_2 catalysts exhibits a single peak centred at about 520 K attributed to the reduction of Cu^{2+} to Cu^0.

Our Cu/SiO_2 catalysts show reduction of copper species centred at 520 and 500 K for the impregnated and sol–gel catalysts, respectively. The observed shift may be due to a different copper particle size, this

Table 1
Specific area, pore volume, percent micropore volume and average pore diameter of 0.5 wt.% Pd–Cu/SiO_2 catalysts

Catalyst	S_{BET} ($m^2\,g^{-1}$)	S_{DRK}[a] ($m^2\,g^{-1}$)	Pore volume ($cm^3\,g^{-1}$)	Micropore volume (%)	Average pore diameter (nm)
Pd(I)/SiO_2	142	–	0.33	1	9.2
Pd–0.3Cu(I)/SiO_2	130	–	0.36	1	11.0
Pd–0.4Cu(I)/SiO_2	127	–	0.32	1	10.0
Pd–0.6Cu(I)/SiO_2	127	–	0.33	1	10.4
Pd–1.2Cu(I)/SiO_2	124	–	0.27	1	8.8
1.0Cu(I)/SiO_2	126	–	0.29	1	9.2
Pd(SG)/SiO_2	–	650	0.43	37	2.4
Pd–0.3Cu(SG)/SiO_2	–	206	0.11	70	2.0
Pd–0.4Cu(SG)/SiO_2	–	382	0.13	84	1.4
Pd–0.6Cu(SG)/SiO_2	–	319	0.12	81	1.5
Pd–1.2Cu(SG)/SiO_2	–	338	0.12	82	1.4
1.0Cu(SG)/SiO_2	–	520	0.20	76	1.5

[a] Specific area calculated by the Dubinin–Radushkewich–Kaganer equation.

being higher in the catalysts prepared by impregnation. In relation to the bimetallic catalysts, the reduction of copper in the series prepared by impregnation takes place at lower temperatures. This is due to the catalytic effect of the small Pd particles, which enhances the reduction of copper oxide, through H_2 dissociation on palladium followed by spillover on the copper oxide phase. The Pd–Cu interactions are expected to be stronger in the region of low copper content, thus making the CuO reduction easier. As the Cu content increases, the temperature reduction peak also increases, being close to the reduction temperature of the monometallic one for the 0.5Pd–1.2Cu/SiO_2 catalyst. For the sol–gel catalyst series, no significant

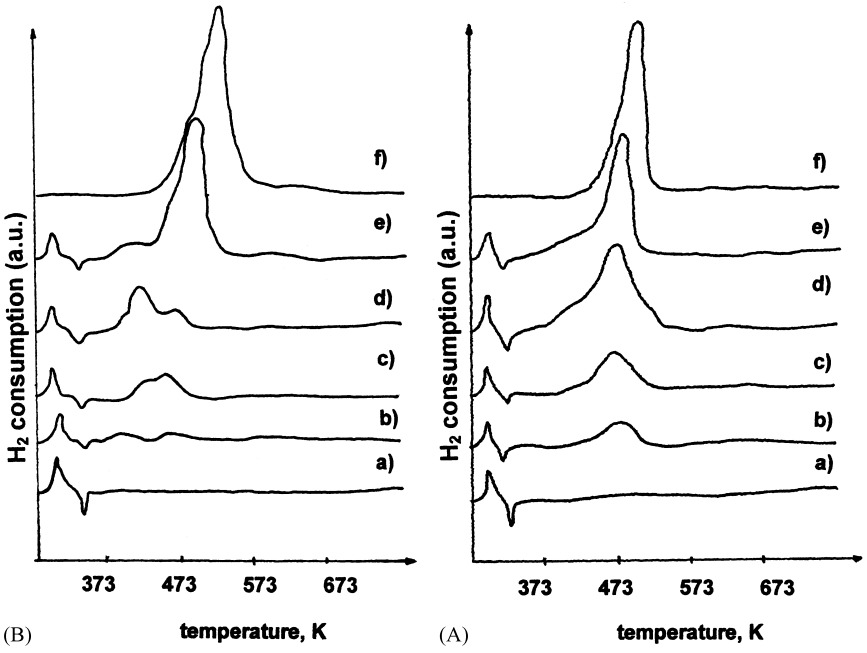

Fig. 2. Temperature-programmed reduction profiles of various Pd–Cu/SiO_2 catalysts: (A) sol–gel series; (B) impregnated catalysts. (a) 0.5Pd/SiO_2; (b) 0.5Pd–0.3Cu/SiO_2; (c) 0.5Pd–0.4Cu/SiO_2; (d) 0.5Pd–0.6Cu/SiO_2; (e) 0.5Pd–1.2Cu/SiO_2; (f) 1.0Cu/SiO_2.

Table 2
H/Pd ratios, metal particle size, binding energies and atomic surface ratios for 0.5 wt.% Pd–Cu/SiO_2 catalysts

Catalyst	H/Pd	d_{TEM} (nm)		BE (eV)		XPS atomic ratios	
		Pd	Cu	Pd $3d_{5/2}$	Cu $2p_{3/2}$	$(Pd/Si)_s$	$(Cu/Si)_s$
Pd(I)/SiO_2	0.46	2.0	–	335.3	–	0.0016	–
Pd–0.3Cu(I)/SiO_2	0.36	1.7	6.0–8.0	335.0	933.3	0.0017	0.0004
Pd–0.4Cu(I)/SiO_2	0.45	1.7	6.0	335.1	933.2	0.0034	0.0011
Pd–0.6Cu(I)/SiO_2	0.51	1.7	6.0–8.0	335.1	933.1	0.0027	0.0018
Pd–1.2Cu(I)/SiO_2	0.44	1.7	4.0	335.2	933.0	0.0038	0.0042
1.0Cu(I)/SiO_2	–	–	4.0	–	933.2	–	0.0025
Pd(SG)/SiO_2	0.74	2.0	–	335.2	–	0.0015	–
Pd–0.3Cu(SG)/SiO_2	0.65	2.0	8.0–10.0	335.0	933.2	0.0019	0.0021
Pd–0.4Cu(SG)/SiO_2	0.58	1.5	8.0–14.0	335.0	933.3	0.0020	0.0016
Pd–0.6Cu(SG)/SiO_2	0.54	1.5	5.0	335.1	933.0	0.0017	0.0027
Pd–1.2Cu(SG)/SiO_2	0.27	1.5	6.0	335.2	933.1	0.0042	0.0061
1.0Cu(SG)/SiO_2	–	–	2.5	–	932.9	–	0.0031

synergetic effect of Pd in the reduction of copper species was noted. This may be explained considering that the H_2-spillover is restricted in these catalysts due to the microporous nature of the support material.

Table 2 summarises the H/Pd ratio, the estimated particle size by H_2-chemisorption and TEM, the XPS binding energies and surface Pd/Si and Cu/Si atomic ratios. Even though CO chemisorption is widely used to evaluate metal dispersion in Pd catalysts, it may be adsorbed linearly or bridgest in different proportion depending on crystal size [19]. H_2-chemisorption may also be used if the precaution to avoid hydrate formation is taken [20] or back-sorption [21]. Thus the H_2-chemisorption is performed at 343 K, the H_2 absorption may be neglected and metal dispersion obtained with this procedure is comparable with that obtained from CO chemisorption data. Metal particle size obtained from H_2-chemisorption at 343 K was evaluated assuming cubic metal particles, in which one face remains on the support and the other five are exposed to hydrogen, by the equation $d = 5/S\rho$. A stoichiometry of $H/Pd_s = 1$ was used. In this equation, S represents the specific metal area and ρ is the metal specific density. In the series prepared by impregnation, almost no changes were detected in Pd dispersion and the particle size was close to 2.0 nm. A decrease in the hydrogen uptake upon increasing copper loading was detected in the catalysts prepared by the sol–gel procedure. This may be due to a partial coverage of Pd particles by copper. This explains the differences observed in the particle size estimated from chemisorption and TEM measurements. Crystal sizes of Pd particles are slightly smaller in this latter series, having particle sizes of approximately 1.5 nm, close to the pore size diameter of the catalysts. Such a catalyst texture has been assumed to be responsible for the resistance to sintering of supported metal catalysts prepared by this method [22]. Copper particles are larger than palladium crystallites by a factor of 2–10, which is expected taking into account the difficulty to get well-dispersed copper particles. The larger size of copper particles than the pore size diameter of the substrate, specially in the sol–gel series, may explain the drop in the H_2 uptake in the catalysts when Cu loading increases.

Fig. 3A and B shows the Pd 3d and Cu $2p_{3/2}$ core-level spectra of the H_2-reduced impregnated catalyst series. Only small changes in the binding energies for Pd $3d_{5/2}$ and Cu $2p_{3/2}$ were found. In the monometallic Pd catalysts, the observed BEs are in agreement with the expected value for Pd^0 [23–25]. Although no significant changes in BE are observed in the Pd–Cu bimetallic catalysts, the full width at half maximum of Pd 3d peaks increased markedly from 3.0 eV in the monometallic Pd sample to 3.6 eV in the bimetallic 0.5Pd–1.2Cu sample, and this increase was less marked at intermediate Pd/Cu compositions. This finding may suggest a Pd–Cu interaction.

In the Pd–Cu/SiO_2 series prepared by impregnation, the slight increase observed in the Pd/Si surface atomic ratio with increasing copper content suggests that Cu may enhance the dispersion of Pd particles or

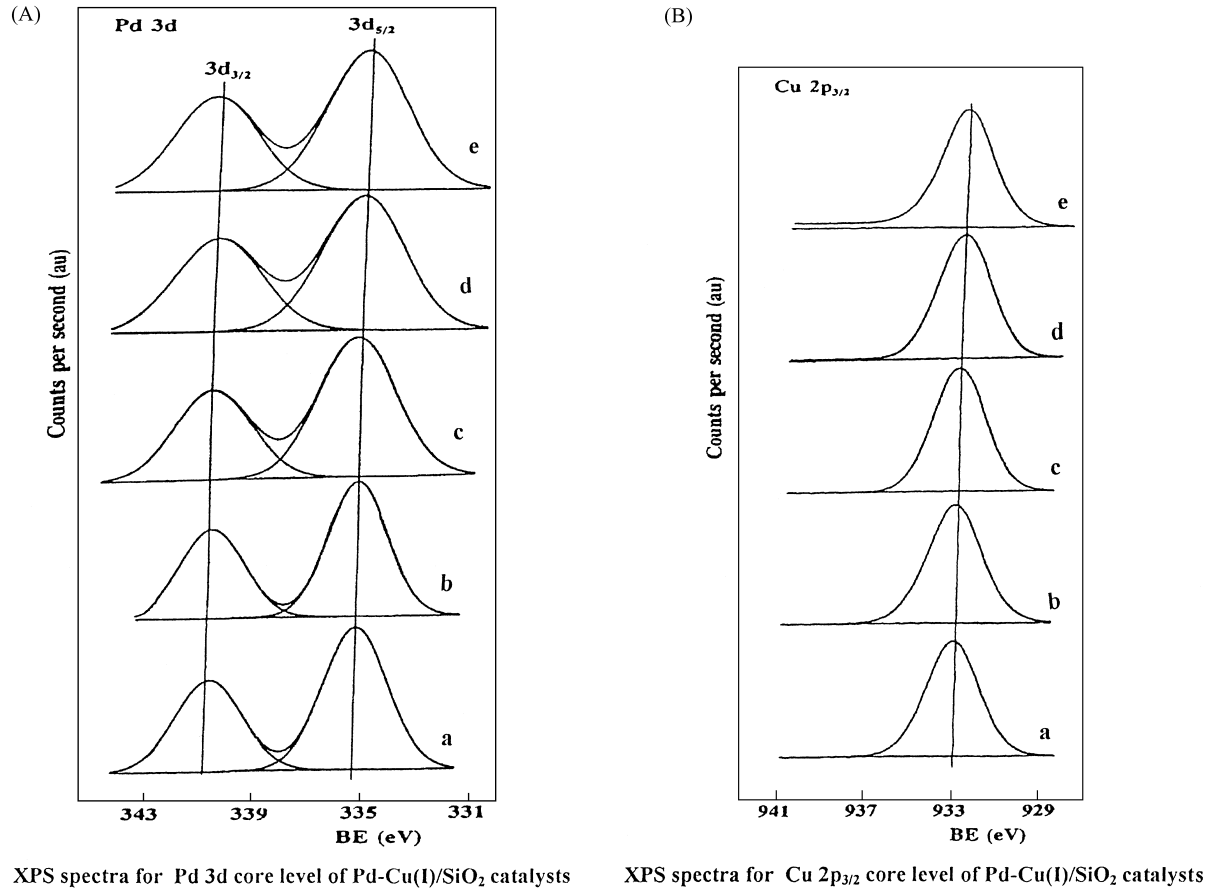

Fig. 3. XPS spectra for Pd–Cu/SiO_2impregnated catalysts: (A) Pd $3d_{5/2}$ core level; (B) Cu $2p_{3/2}$ core level. (a) 0.5Pd/SiO_2 or 1.0Cu/SiO_2; (b) 0.5Pd–0.3Cu/SiO_2; (c) 0.5Pd–0.4Cu/SiO_2; (d) 0.5Pd–0.6Cu/SiO_2; (e) 0.5Pd–1.2Cu/SiO_2.

because of a surface coverage of silica by copper. The Pd/Si ratio increases with Cu loading in similar proportion compared with the copper loading, indicating similar copper dispersion, in agreement with TEM results. In the sol–gel series, Pd/Si ratio also increases with increasing copper content, although it follows a complex dependence. This is probably due to the fact that the specific area of the catalysts are also different.

The activity data for methane oxidation as a function of the reaction temperature up to complete combustion for one series of the catalysts is shown in Fig. 4. In this figure, typical sigmoidal curves can be seen in which the reaction starts at about 550 K, then the conversion increases drastically as the temperature increases and a complete conversion is reached. Carbon dioxide and water were the main products of the reaction, however, at high conversion levels (>60%) traces of CO were also detected. Differences in the conversion level at a given temperature for catalysts having different Cu content are observed. In fact, as copper loading increases the curve shifts towards higher temperatures indicating lower activity.

In order to compare the activity per active site, turnover frequencies (TOFs), expressed as number of methane molecules converted per Pd surface atom per second, for methane oxidation at 623 K were calculated. The TOF values are shown in Table 3. The bimetallic impregnated catalysts have almost the same TOF, which are lower than for the monometallic palladium catalyst. This may be attributed to a change in the nature of the active sites produced by the copper addition and not to a partial coverage of Pd particles,

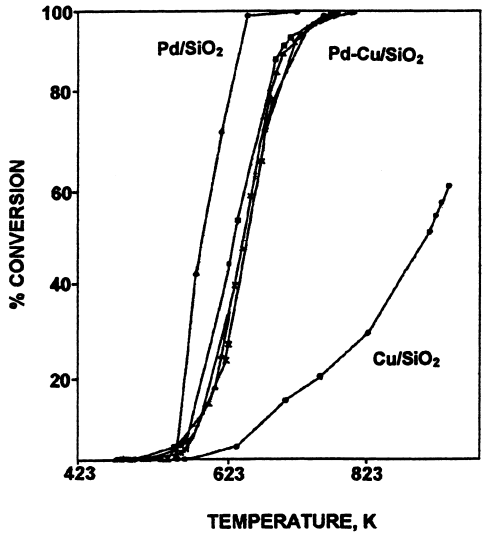

Fig. 4. Catalytic activity in the combustion of methane for impregnated Pd–Cu/SiO_2 series.

as quantitative XPS data suggest. In the sol–gel series, the monometallic Pd/SiO_2 catalyst has higher TOF than the bimetallic Pd–Cu catalysts, which can be explained considering that the monometallic has an important proportion of mesoporosity, which is absent in the bimetallic catalysts. In the bimetallic catalysts the access of the reactants to the active site is limited. This interpretation also explains the activity differences observed in both series of catalysts. The ignition temperature (T_i^{50}), defined as the temperature required to obtain a 50% CH_4 conversion in different conditions under stoichiometric and oxidant conditions are compiled in Table 3. In both catalyst series the ignition temperature is lower for the monometallic Pd catalysts, whereas in the bimetallic Pd–Cu system this value is almost constant.

Comparison of catalytic activity of the impregnated and the sol–gel catalysts indicated that the activity is high in all the impregnated catalysts. As metal dispersion is even lower in the impregnated catalysts (Table 2), but specific areas are higher in the sol–gel catalysts as a consequence of their microporosity (Table 1), this behaviour appears to be related to differences in accessibility of the reactants to the active site. As expected, for all the catalysts, the ignition temperature is lower in excess of oxygen in the feed.

In order to study the resistance to sintering of all the prepared catalysts, they were subjected to sintering. The sintering treatment consists of: (i) maintaining the catalysts under stoichiometric conditions of reaction up to 923 K for 10 h; (ii) cooling down to 673 K, shifting the reactant mixture to He for 30 min, switching to pure hydrogen; reducing again at 773 K for 2 h; (iii) conducting a new combustion cycle. Fig. 5 shows the combustion of methane under stoichiometric conditions for a representative catalysts, under different treatments of the catalyst. When a new catalytic cycle is carried out on the used catalyst, the second cycle exhibits the same behaviour, however, an increase in the activity is produced. In the sol–gel series, the

Table 3
Catalytic activity of 0.5 wt.% Pd–Cu/SiO_2 catalysts in methane combustion

Catalyst	T_i^{50} (K)			TOF at 623 K
	Stoichiometric	Oxidant	Sintering	
Pd(I)/SiO_2	593	575	590	0.101
Pd–0.3Cu(I)/SiO_2	643	625	670	0.074
Pd–0.4Cu(I)/SiO_2	653	640	680	0.050
Pd–0.6Cu(I)/SiO_2	653	637	683	0.043
Pd–1.2Cu(I)/SiO_2	653	633	685	0.047
1.0Cu(I)/SiO_2	903	905	970	–
Pd(SG)/SiO_2	673	605	593	0.162
Pd–0.3Cu(SG)/SiO_2	763	760	705	0.033
Pd–0.4Cu(SG)/SiO_2	793	770	740	0.024
Pd–0.6Cu(SG)/SiO_2	783	790	738	0.026
Pd–1.2Cu(SG)/SiO_2	793	803	742	0.051
1.0Cu(SG)/SiO_2	873	900	840	–

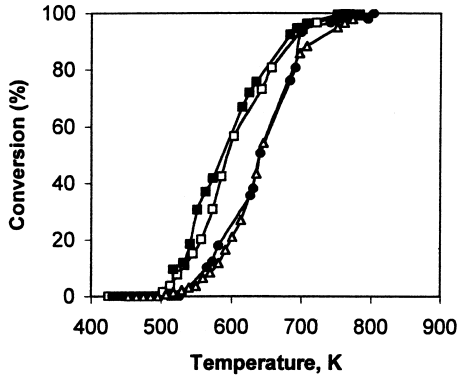

Fig. 5. Catalytic activity under stoichiometric conditions in the combustion of methane for 0.5% Pd(I)/SiO_2. (△) Calcined sample; (□) reduced sample; (■) used sample; (●) sintered sample.

trend was similar to that previously described except in the behaviour of the catalysts after the sintering treatment. In this case, the catalysts were even more active than the reduced and used ones. In all the impregnated catalysts, it was found a slight decrease in the conversion levels mainly in the bimetallic Pd–Cu catalysts, whereas in those obtained by the sol–gel method, the activity increased. The change in the activity in the impregnated catalyst series is attributed to a sintering in the metal component. In fact, TEM revealed an increase in the metal particle size of both Pd and Cu crystals. Nevertheless, the TOF obtained for these catalysts is higher due to the increase in the metal particle size. In the sol–gel series, almost no changes were detected in Pd particle size, but a slight increase in Cu particle was observed. Besides, a significant development of mesoporosity of the catalyst, in this latter catalyst series, seems to be responsible of the changes in the activity. Thus, after sintering, the specific area of Pd/SiO_2(SG) drops from 650 to 442 $m^2\,g^{-1}$ and the proportion of micropores decreases from 37 to 5%. Similar trends were found in all the sol–gel catalysts, but in the Pd–Cu bimetallic samples, a significant proportion of micropores is still present, limiting the access to the active sites, which may explain the lower TOF of the sol–gel catalysts as compared with the impregnated counterpart.

This feature has also been reported previously for Pd supported catalysts [26,27] and has been attributed to a partial oxidation of the metal cluster leading to more active species than the reduced sample. The catalytic behaviour of the calcined and unreduced Pd/SiO_2 sample displays a similar trend, although it is less active than the reduced or used catalyst, thus confirming that the Pd^{2+} is not the active site. The activity of the unreduced catalyst after the sintering procedure, is almost coincident with that of the oxidised sample of the impregnated series. This behaviour can be attributed to a decrease in the number of active sites by agglomeration of metal particles.

4. Conclusions

The influence of different variables of preparation of Pd/SiO_2, $Pd–Cu/SiO_2$ and Cu/SiO_2 catalysts series on their surface and the catalytic properties were studied. The procedure to deposit the metal component (by impregnation or sol–gel) and the nature of the metal precursor modifies the porosity and the specific area in the catalysts prepared by the sol–gel method, whereas almost no change was detected in the impregnated catalyst series. With regard to the nature of the metal precursor, the presence of ionic compounds during the gelation process led to the development of microporosity of the solids prepared by the sol–gel procedure. Palladium metal dispersion is comparable in all the studied catalysts, with palladium crystal sizes ranging from 1.5 to 2.0 nm. Copper particles are larger and most of them are in the range from 6 to 10 nm.

The activity in the combustion of methane depends mainly on the accessibility of the reactant to the palladium active sites. Thus, in the impregnated catalysts, activity decreases as copper loading increases, which is attributed to Pd–Cu interaction. In the sol–gel catalysts, activity of all the catalysts is lower than for the impregnated counterparts due to differences in catalyst texture. The presence of microporosity limits the access of the reactants to the active site in the former catalysts. The impregnated catalysts when subjected to stringent reaction conditions suffer a slight deactivation by sintering of metal particles, whereas in the sol–gel catalysts activity increased with respect to the fresh samples. This behaviour is explained in terms of the textural changes of the catalysts upon the treatments. In fact, a decrease in specific area and extent of micropores contribution, and an increase of mesoporosity, in the sol–gel catalysts were observed.

Acknowledgements

The authors thank CONICYT (Grant FONDECYT No. 1990484) for the financial support.

References

[1] R. Prassad, L. Kennedy, E. Ruckenstein, Catal. Rev. Sci. Eng. 26 (1984) 1.
[2] G. Pecchi, P. Reyes, I. Concha, J.L.G. Fierro, J. Catal. 179 (1998) 309.
[3] R.B. Anderson, K.C. Stein, J.J. Feenan, L.E.J. Hofer, Ind. Eng. Chem. 53 (1961) 809.
[4] P.O. Larsson, H. Berggren, A. Anderson, O. Augustsson, Catal. Today 35 (1997) 137.
[5] C.F. Cullis, B.M. Willat, J. Catal. 83 (1983) 267.

[6] T.R. Baldwin, R. Burch, Appl. Catal. 66 (1990) 359.
[7] C.U. Odenbrand, S.L. Andersson, L.A. Andersson, O. Augustsson, J.G. Brandin, G. Busca, J. Catal. 125 (1990) 541.
[8] H. Widjaja, K. Sekisawz, K. Eguchi, H. Arai, Catal. Today 35 (1997) 197.
[9] J.A.A. van den Tillaart, J. Leyrer, S. Eckhoff, E.S. Lox, Appl. Catal. B 10 (1996) 53.
[10] P. Reyes, M. Morales, G. Pecchi, Bol. Soc. Chil. Quím. 41 (1996) 221.
[11] T. López, A. Romero, R. Gómez, J. Non-Cryst. Solids 127 (1991) 105.
[12] P. Reyes, A. Figueroa, G. Pecchi, J.L.G. Fierro, unpublished results.
[13] G. Pecchi, M. Morales, P. Reyes, React. Kinet. Catal. Lett. 61 (1997) 237.
[14] C.D. Wagner, L.E. Davis, M.V. Zeller, J.A. Taylor, R.H. Raymond, L.H. Gale, Surf. Interf. Anal. 3 (1981) 211.
[15] T. López, React. Kinet. Catal. Lett. 46 (1992) 45.
[16] K.-i. Muto, N. Katada, M. Niwa, Appl. Catal. A 134 (1996) 203.
[17] V. Ragaini, R. Giannantonio, P. Magni, L. Lucarelli, G. Leofanti, J. Catal. 146 (1994) 116.
[18] S.D. Robertson, B.D. McNicol, J.H. de Baas, S.C. Kloet, J.W. Jenkins, J. Catal. 37 (1975) 424.
[19] J.R. Anderson, K.C. Pratt, Introduction to Characterization and Testing of Catalysts, Academic Press, New York, 1985 (Chapter I).
[20] P.C. Aben, J. Catal. 10 (1968) 224.
[21] J.E. Benson, H.S. Hwang, M. Boudart, J. Catal. 30 (1973) 146.
[22] T. López, P. Bosch, M. Asomoza, E. García-Figueroa, R. Gómez, J. Catal. 138 (1992) 463.
[23] N. Iwasa, S. Masuda, O. Ogawa, N. Takezawa, Appl. Catal. A 125 (1995) 145.
[24] A.M. Venezia, A. Rossi, D. Duca, A. Martorana, G. Deganello, Appl. Catal. A 125 (1995) 113.
[25] J. Goetz, M.A. Volpe, A.M. Sica, C.E. Gigola, R. Touroude, J. Catal. 153 (1995) 86.
[26] R.J. Farrauto, M.C. Hobson, T. Kennelly, E.M. Waterman, Appl. Catal. A 81 (1992) 27.
[27] J.G. McCarty, Catal. Today 26 (1995) 283.